

Examination of Diffusion Process for High-speed Avalanche Photodiode Fabrication

Ilgu Yun *, Kyung-Sook Hyun**, Yong-Hwan Kwon** and Kwang-Eui Pyun**

Abstract

The characterization of zinc diffusion processes applied for high-speed avalanche photodiodes has been examined. The different diffusion process conditions for InP test structures were explored. The zinc diffusion profiles, such as the diffusion depth and the zinc dopant concentration, were examined using secondary ion mass spectrometry with varying the process variables and material parameters. It is observed that the diffusion profiles are severely impacted on the process parameters, such as the amount of Zn_3P_2 source and the diffusion time, as well as material parameters, such as doping concentration of diffusion layer. These results can be utilized for the high-speed avalanche photodiode fabrication.

Keywords : diffusion process , optoelectronic devices , semiconductor manufacturing.

1. Introduction

The diffusion process is widely used for fabricating in InP-based electronic and optoelectronic devices, such as avalanche photodiodes (APDs) [1]. For the application of 1.55- μ m wavelength high-speed fiber-optic communication system, the planar InP/InGaAs avalanche photodiode with floating guard ring is one of the potential candidates for receiver module [2]. In order to construct the p-n junction of the APDs, the diffusion process is a preferred technique because it can be formed highly doped p-region. Since zinc diffuses one to two orders of magnitude faster than the other

dopants like cadmium, one of the biggest challenges associated with the use of zinc as a diffused dopant in InP is the control of diffusion [3]. In addition, the diffusion profile distribution determined junction curvature which can significantly impact on the edge breakdown [4]. Therefore, the precise control and modeling of diffusion depth and diffused dopant concentration is required to apply this technique for the high-speed avalanche photodiode fabrication [5-7].

In this paper, the characterization of two different InP-based test structures (InP/InGaAs epitaxial structure, and n-type InP substrate) are presented and the results of diffusion process for two test structures are compared and analyzed. These two test structures are mainly distinguished by the doping concentration of the diffused layer. The zinc diffusion profiles, such as the diffusion depth and the zinc dopant concentration, were

* : Dept. of Electrical & Electronic Eng., Yonsei Univ., 134 Shinchon-dong, Seodaemun-ku, Seoul, Korea (E-mail: iyun@yonsei.ac.kr) (Tel:2123-4619; Fax: 362-6444)

** : ETRI, 161 Kajung-dong, Yusung-ku, Taejon, Korea

2000년 8월 29일 접수, 2000년 10월 4일 심사완료.

examined using secondary ion mass spectrometry with varying the amount of Zn_3P_2 source, the ampoule volume, and the diffusion time. The Zn diffusion processes were performed via sealed ampoule technique using pumping system and diffusion furnace [8]. The diffused Zn profiles were measured with secondary ion mass spectrometry (SIMS) using a Cs^+ beam and detecting the $CsZn^+$ cluster at mass 197 in a Cameca IMS-4F instrument [9].

2. Test Structure Description

The first test structure is an InP/InGaAs epitaxial structure. This test structure were grown by the metal organic chemical vapor deposition (MOCVD) growth technique at Electronics and Telecommunications Research Institute. It is composed of a basic p-i-n structure with inserting grading and buffer layers. The schematic cross section of InP/InGaAs test structure is illustrated in Figure 1 and the thicknesses and doping concentrations of InP/InGaAs epitaxial layers are summarized in Table 1.

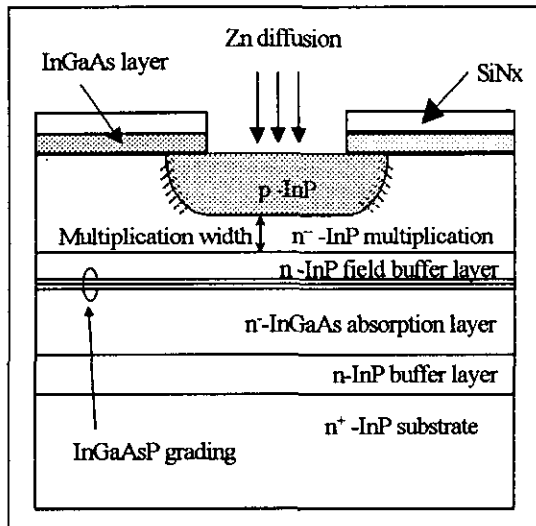


Fig. 1 Schematic diagram of InP/InGaAs test structure

The p-region is constructed by zinc diffusion process on the 3.5- μm thick undoped multiplication region. In addition, the 2000- \AA thick SiN_x passivation layer is added on the top for diffusion pattern and 1500- \AA thick InGaAs layer is added just below the passivation layer to suppress the lateral diffusion. In order to obtain the required characteristics for high-speed applications, the total charge density of the charge plate and multiplication layer thickness should be precisely controlled [10]. The second test structure is S-doped n-type ($1 \times 10^{18} \text{cm}^{-3}$) InP substrate and the third test structure is the undoped InP substrate which is unintentionally doped n-type at about 10^{15}cm^{-3} .

Table 1 Summary of InP/InGaAs epitaxial layer structure

Layer Name	Material	Thickness [μm]	Doping [cm^{-3}]
Multiplication	n ⁻ -InP	3.5	5.0×10^{16}
Field buffer	n-InP	0.2	1.5×10^{17}
Grading 1	u-InGaAsP (1.1Q)	0.03	2.0×10^{15}
Grading 2	u-InGaAsP (1.3Q)	0.03	2.0×10^{15}
Grading 3	u-InGaAsP (1.5Q)	0.02	2.0×10^{17}
Absorption	u-InGaAs	1.0	2.0×10^{15}
Buffer	n-InP	1.0	1.0×10^{18}
Substrate	n ⁺ -InP	350	2.0×10^{18}

Prior to the diffusion process, these test structures were cleaned and slightly etched to remove surface damage. In addition, the zinc diffusion depth is defined as the depth where Zn dopant concentration is 1×10^{17} atoms/cc.

3. Experimental Setup and Measurement

The zinc diffusion processes were performed via sealed ampoule technique using diffusion furnace maintaining temperature at about 495

°C in flowing N₂ gases with varying the process conditions. Figure 2 shows the schematic diagram for diffusion furnace. The ampoule in a quartz boat was loaded in the pre-heating zone and waited for 10 minutes before diffusion. After diffusion process, the ampoule was pulled out of diffusion furnace and cooled rapidly by dropping it into water. Then, Zn diffusion profiles were measured with secondary ion mass spectrometry (SIMS) using a Cameca-IMS 4F instrument. A 5.5 keV Cs⁺ primary ions were used. The CsZn⁺ ions were detected to monitor the Zn concentration. The sputtering rate was deduced by measuring the depth of the ion-impacted crater, which can extrapolate the diffusion depth, and a Zn-doped bulk InP sample was used to calibrate the concentration.

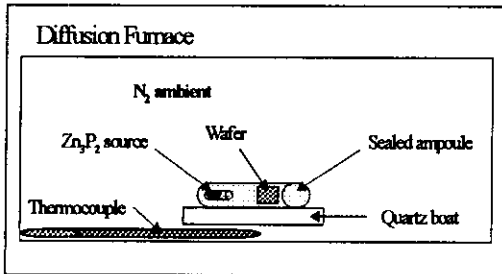


Fig. 2 Schematic diagram of diffusion furnace

4. Results and Discussions

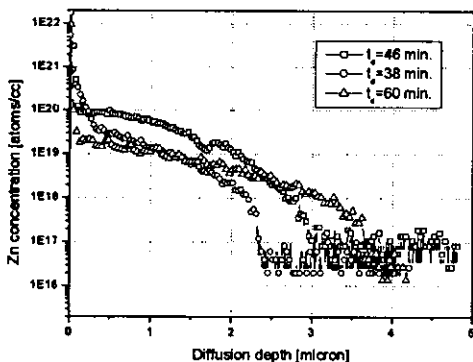


Fig. 3 SIMS profiles for the InP/InGaAs epitaxial structures

Figure 3 represents SIMS depth profiles for the Zn concentration in the InP/InGaAs test structures. Here, the ampoule pressure holds constant for three test structures. The diffusion process condition for these test structures is summarized in Table 2. From these results, the diffusion depth can be extrapolated. The diffusion depths of three test structures diffused in 38 min., 46min., and 60 min. are 2.41 μm, 3.06 μm, and 3.74 μm, respectively. It can also be seen that the Zn concentration distribution is dependent on the amount of Zn₃P₂ source. However, it does not significantly impact on the diffusion depth. In order to obtain certain Zn concentration distribution, the amount of Zn₃P₂ source can be determined by the volume of the ampoule.

Table 2 Process condition for InP/InGaAs epitaxial structures

	Ampoule Size [cc]	Amount of Zn ₃ P ₂ [mg]	Diffusion time [min]
Sample #1	8	50	38
Sample #2	8	75	46
Sample #3	22	150	60

The similar results can be obtained from the SIMS depth profiles for the Zn concentration in the n-type substrate test structures. The diffusion depths of four test structures diffused in 41 min., 43 min., 46min., and 60 min. are 1.3 μm, 1.36 μm, 1.41 μm and 1.61 μm, respectively. Compared with the results from the InP/InGaAs epitaxial structures, it can be explained that the range of the diffusion depth has narrow boundary as the doping concentration of the layer for the diffusion is increased. SIMS depth profiles for the Zn concentration in the n-type InP substrate test structures are shown in Figure 4.

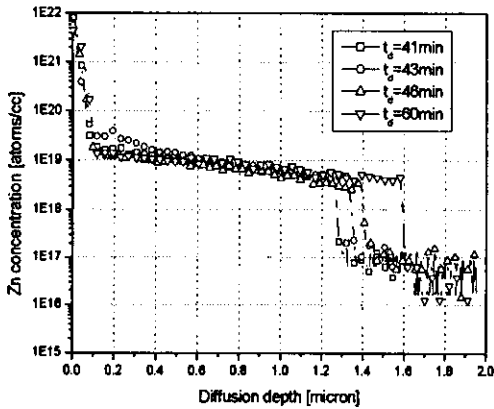


Fig. 4 SIMS profiles for the n-type InP substrates

In addition, SIMS depth profiles for the Zn concentration in different test structures are shown in Figure 5. Four test samples are used to obtain SIMS profile of n-type InP substrates with varying the diffusion time.

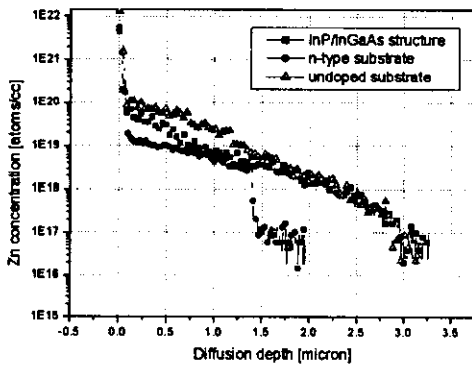


Fig. 5 SIMS profiles for three different test structures

Undoped InP substrate sample is diffused for 40 minutes and InP/InGaAs epitaxial structure sample and n-type InP substrate sample are diffused for 46 minutes each. It is examined that the diffusion profile of n-type substrate is very abrupt compared with other test structures. Since the major difference between the test structures is the doping concentration of diffused layer, it can be presented that diffusion

profile and diffusion rate is significantly impacted on the status of doping concentration of diffused InP layer. It is also observed that undoped InP substrate sample exhibit the highest diffusion rate among the test structures.

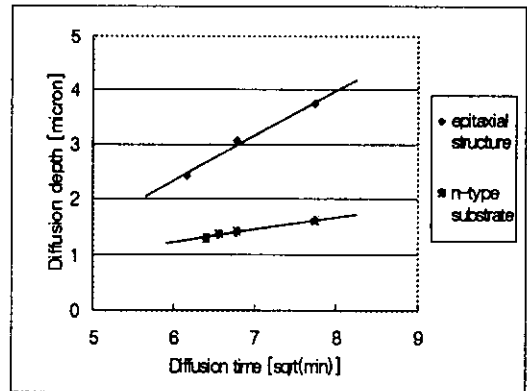


Fig. 6 Diffusion depth as a function of the square root of the diffusion time

The plots of the Zn diffusion depth versus the square root of the diffusion time for InP/InGaAs structures and n-type substrates are presented in Figure 6. The diffusion depth versus the square root of the diffusion time yields a linear relationship as expected for a classical diffusion process. The data for sealed ampoule diffusion matches modeled data quite well, indicating that diffusion process characterization can reproducibly be performed using a simple classical diffusion model. Moreover, it is noted that that diffusion rates for epitaxial layer and n-type substrate are $0.829 \text{ m/min}^{1/2}$ and $0.222 \text{ m/min}^{1/2}$, respectively. It is found that higher doping concentration in diffused layer before diffusion process can create more abrupt junction and the diffusion depth can be controlled more precisely.

5. Conclusion

In summary, the Zn diffusion process of three different test structures, InP/InGaAs epitaxial structure, n-type InP substrate, and undoped

InP substrate, has been investigated using sealed ampoule technique. The results show that the Zn diffusion depth and concentration can be reproducible if the process parameters, such as the amount of Zn₃P₂ source, the ampoule pressure, the ampoule size, and the diffusion time, are carefully controlled and optimized. These experimental results can be utilized for the fabrication of long-wavelength high-speed avalanche photodiodes for optical communication system application.

Acknowledgments

The authors would like to thank Y. K. Kim for her aid in performing SIMS measurements. We are also grateful to J. S. Kim for many helpful discussions.

References

- [1] Y. Liu, S. R. Forrest, J. Hladky, M. J. Lange, G. H. Orsen, D. E. Ackley, "A planar InP/InGaAs avalanche photodiode with floating guard ring and double diffused junction," *J. lightwave tech.* vol. 10, no. 2, 1992, pp. 182-193.
- [2] T. Y. Yun, M. S. Park, J. H. Han, I. Watanabe, K. Makita, "10-Gigabit-per-second High-sensitivity and Wide-dynamic-range APD-HEMT Optical Receiver," *IEEE Photonic. Tech. Lett.*, vol. 8, no. 9, 1996, pp. 1232-1234.
- [3] V. Swaminathan, C. L. Reynolds, Jr., M. Geva, "Zn diffusion behavior in InGaAsP/InP capped mesa buried heterostructures," *Appl. Phys. Lett.*, vol. 66, no. 20, 1995, pp. 2685-2687.
- [4] S. M. Sze, G. Gibbons, "Effect of junction curvature on breakdown voltage in semiconductors," *Solid-State Electron.*, vol. 9, 1966, pp. 831-845.
- [5] 정형섭, 이종근, 박세근, 양재균, "고밀도 산소 플라즈마를 이용한 감광제 제거공정에 관한 연구," 한국전기전자재료학회논문지, vol. 11, no.2, pp. 95-100, 1998.
- [6] 김경섭, 신영의, "Retrograde Well 형성을 위한 고에너지 이온주입에 대한 연구," 한국전기전자재료학회논문지, vol. 11, no. 5, pp. 358-364, 1998.
- [7] 이수부, 박헌건, 이석현, "유도결합형 플라즈마 원을 이용한 고선택비 산화막 식각에 관한 연구," 한국전기전자재료학회논문지, vol.11, no. 4, pp. 261-265, 1998.
- [8] G. J. van Gorp, T. van Dongen, G. M. Fontijn, J. M. Jacobs, D. L. A. Tjaden, "Interstitial and Substitutional Zn in InP and InGaAsP," *J. Appl. Phys.* vol. 65, no. 2, 1989, pp. 553-560.
- [9] C. Blaauw, F. R. Shepherd, D. Eger, "Secondary Ion Mass Spectrometry and Electrical Characterization of Zn Diffusion in n-type InP," *J. Appl. Phys.*, vol.66, no.2, 1989, pp. 605-610.
- [10] K. Hyun, C. Park, "Breakdown Characteristics in InP/InGaAs Avalanche Photodiode with p-i-n Multiplication Layer Structure," *J. Appl. Phys.*, vol. 81, no. 2, 1997, pp. 974-984.